

## Triplet Exciton Diffusion and Phosphorescence Quenching in Iridium(III)-Centered Dendrimers

J. C. Ribierre,<sup>1</sup> A. Ruseckas,<sup>1</sup> K. Knights,<sup>2</sup> S. V. Staton,<sup>2</sup> N. Cumpstey,<sup>2</sup> P. L. Burn,<sup>2,3</sup> and I. D. W. Samuel<sup>1</sup>

<sup>1</sup>*Organic Semiconductor Centre, SUPA, School of Physics and Astronomy, University of St. Andrews, North Haugh, St. Andrews, Fife KY16 9SS, United Kingdom*

<sup>2</sup>*Department of Chemistry, University of Oxford, Chemistry Research Laboratory, Mansfield Road, OX1 3TA Oxford, United Kingdom*

<sup>3</sup>*Centre for Organic Photonics and Electronics, School of Molecular and Microbial Science, Chemistry Building, University of Queensland, Queensland, 4072, Australia*

(Received 30 May 2007; published 10 January 2008)

A study of triplet-triplet exciton annihilation and nonradiative decay in films of iridium(III)-centered phosphorescent dendrimers is reported. The average separation of the chromophore was tuned by the molecular structure and also by blending with a host material. It was found that triplet exciton hopping is controlled by electron exchange interactions and can be over 600 times faster than phosphorescence quenching. Nonradiative decay occurs by weak dipole-dipole interactions and is independent of exciton diffusion, except in very thin films (<20 nm) where surface quenching dominates the decay.

DOI: [10.1103/PhysRevLett.100.017402](https://doi.org/10.1103/PhysRevLett.100.017402)

PACS numbers: 78.66.Qn, 73.50.Gr, 78.40.Me, 78.55.Kz

Excitation energy transfer is an important process in organic semiconductors and has to be taken into account when designing new optoelectronic materials and devices. In photovoltaic devices, the neutral excited state is generated by light absorption and must diffuse to a heterojunction with another material to be separated into charge carriers and so provide photocurrent. In organic light emitting diodes (OLEDs), exciton diffusion can lead to a decrease of the electroluminescence efficiency due to quenching of the emitting state by intermolecular interactions and defects [1,2], exciton interactions with charge carriers [2,3], and exciton-exciton annihilation [4,5]. These quenching effects are more pronounced in phosphorescent OLEDs than in fluorescent devices because of the longer excited state lifetime. Nevertheless, phosphorescent OLEDs show much higher internal quantum efficiencies due to their ability to convert both singlet and triplet excitons into light [6–8]. A photoluminescence (PL) study of iridium(III) complexes dispersed into a wide energy gap host suggested that intermolecular quenching of phosphorescence in films is controlled by the dipole-dipole interactions between emitters [9]. However, the impact of exciton migration on phosphorescence quenching has not been considered.

In this Letter, we compare the dynamics of triplet exciton diffusion and quenching in several *fac*-tris(2-phenylpyridyl)iridium(III) [Ir(ppy)<sub>3</sub>]-cored phosphorescent dendrimers. Dendrimers provide a convenient way of changing the spacing of the core chromophores in the solid state and hence of studying the effect of spacing on the physics of exciton diffusion and light emission. The triplet exciton diffusion rates are extracted from the measurements of triplet-triplet annihilation and have an exponential dependence on chromophore spacing. This shows that diffusion is controlled by nearest-neighbor electron exchange interactions [10]. Nonradiative decay in 180 nm thick films is governed by much weaker dipole-dipole

interactions and does not depend on the triplet diffusion rate. In much thinner films (<20 nm), phosphorescence quenching is found to depend on exciton diffusion and can be modeled using the diffusion equation together with quenching at the film surface.

Five green Ir(ppy)<sub>3</sub>-cored dendrimers were used in this study and their chemical structures are shown in the insets of Fig. 1. They were studied as neat films, and their different structures give a range of chromophore spacings. In addition to being studied as a neat film, the first generation IrG1 dendrimer was also blended into a 4,4'-bis(*N*-carbazolyl)biphenyl (CBP) or *m*-bis(*N*-carbazolyl)benzene (mCP) host at various concentrations, providing an additional way of tuning the spacing between the dendrimer cores. Dendrimer films were deposited by spin-coating onto precleaned quartz substrates from chloroform solutions. Film thickness was determined by spectroscopic ellipsometry. The film photoluminescence quantum yield (PLQY) was measured in an integrating sphere [11] under a flowing nitrogen atmosphere using a helium-cadmium laser with a wavelength of 325 nm and a power of ~0.2 mW. PL kinetics were measured by the time-correlated single-photon counting technique. For exciton-exciton annihilation measurements, 170–200 nm thick films were excited with the 3rd harmonic of a pulsed Nd:YAG laser at a wavelength of 355 nm. The excitation light at a repetition rate of 10 kHz was focused onto a spot of 0.3 mm diameter. The emitted light was dispersed in a monochromator and detected with a cooled Hamamatsu microchannel plate photomultiplier tube RU-3809U-50. Measurements were performed at the wavelength corresponding to the maximum of the PL spectrum of our samples and in a vacuum of <8 × 10<sup>-4</sup> mbar. PL kinetics at low excitation density were identical to those measured after excitation at 395 nm with a Picoquant pulsed laser diode, which was used for thickness-dependent PL studies.

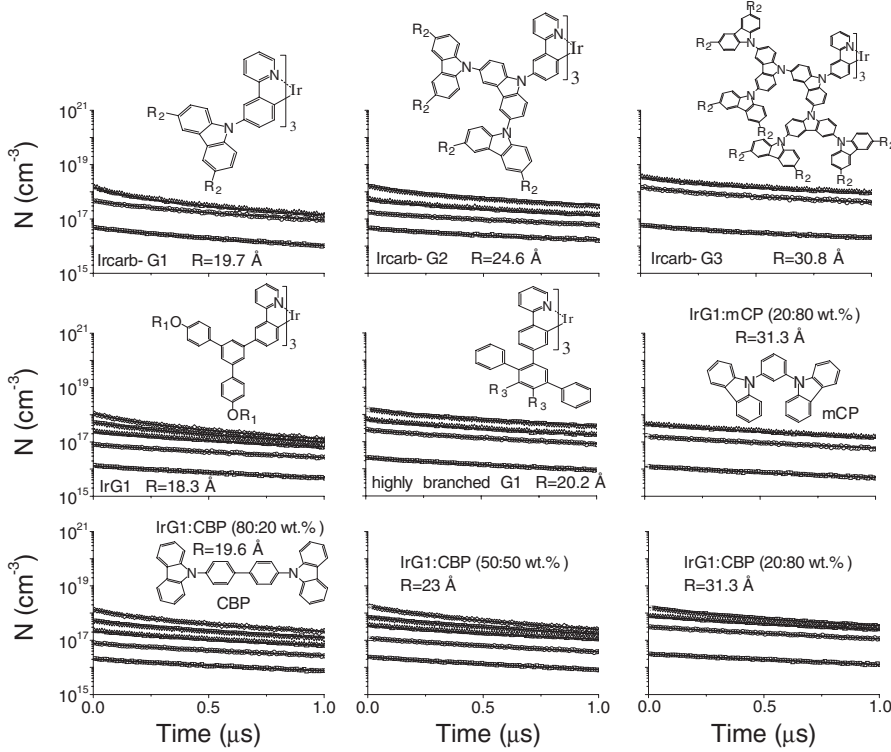


FIG. 1. Intensity dependent PL kinetics of several phosphorescent dendrimers. Solid lines are the fits calculated using Eq. (1). The chemical structure of the dendrimers used in this work and their estimated diameter  $R$  are given in the insets.  $R_1 = 2$ -ethylhexyl,  $R_2 = (9,9$ -di- $n$ -propylfluoren-2-yl), and  $R_3 = 4$ -(9,9-di- $n$ -propylfluoren-2-yl)phenyl.

Figure 1 shows the PL kinetics measured at different initial excitation densities  $N_0$ , which were calculated from the absorption and the incident laser energy density. PL decays are independent of excitation density for  $N_0 < 2 \times 10^{17} \text{ cm}^{-3}$ . At higher excitation densities, phosphorescence decays faster because of triplet-triplet annihilation [4,5,12,13]. The density of triplet excitons  $N$ , which is directly proportional to the PL intensity, can be described by the rate equation:  $dN/dt = -N/\tau - \gamma N^2$ , where  $\tau$  is the exciton lifetime at low excitation density and  $\gamma$  is the annihilation rate, which represents the encounter rate of excitons. In the case of time independent  $\gamma$ , the solution is

$$N(t) = \frac{N_0 \exp(-t/\tau)}{1 + \gamma \tau N_0 [1 - \exp(-t/\tau)]}. \quad (1)$$

We analyzed the decays for the time interval of  $t < 0.5 \mu\text{s}$  where decays are exponential at low excitation density. All the PL decays fit well with Eq. (1) and the  $\gamma$  values are plotted in Fig. 2(a) as a function of the center-to-center distance between phosphorescent molecules  $R$ . This intermolecular spacing was calculated by considering the molecules as hard spheres and using a film density of  $1.1 \text{ g/cm}^3$ . Neutron reflectivity measurements gave a film density for Ir(ppy)<sub>3</sub> cored dendrimers ranging from  $1.06$  to  $1.14 \text{ g/cm}^3$  with about 10% uncertainties. The  $\gamma$  values strongly decrease with increasing  $R$  and the dependence on interchromophore distance is exactly the same in neat films and in the IrG1 blends. This indicates that both the dilution of the phosphorescent emitters into a suitable host and the dendritic structure offer the possibility to

finely control the exciton annihilation rate and thus the exciton diffusion processes.

In the case of a diffusion controlled annihilation in 3D, the annihilation rate  $\gamma$  is related to the exciton diffusion constant  $D$  by:  $\gamma = 4\pi DR_a$ , where  $R_a$  is the reaction radius at which annihilation is faster than hopping and can be taken as  $R$ . Because of fast exciton dephasing, exciton diffusion occurs by incoherent hopping and in a 3D system  $D$  is related to the nearest-neighbor hopping rate,  $k_h$ , by:  $D = R^2 k_h / 3$  [14]. In Fig. 2(b),  $k_h$  is found to decrease exponentially with increasing  $R$  in the range of 1.8 to 3.2 nm, indicating that diffusion is by an electron exchange interaction. Our experimental data were fitted by:

$$\ln k_h = \ln k_h^0 - \beta(R - R_v), \quad (2)$$

where  $\beta$  and  $k_h^0$  are an attenuation factor and the hopping rate at the van der Waal's distance  $R_v$ . The best fit gives  $\beta = 0.33 \text{ \AA}^{-1}$  and  $k_h^0 = 4 \times 10^9 \text{ s}^{-1}$  at  $R_v = 1 \text{ nm}$ .

The PLQY values and the PL lifetime  $\tau$ , obtained from the low excitation density kinetics by fitting them to single exponential decay, increase with  $R$  [Fig. 2(c)]. We calculated the radiative and nonradiative decay rates  $k_R$  and  $k_{NR}$  using  $\text{PLQY} = k_R / (k_R + k_{NR})$  and  $1/\tau = k_R + k_{NR}$ . For IrG1 blends,  $k_R$  is independent of the spacing and equal to  $7 \times 10^5 \text{ s}^{-1}$  which is within 10% of the reported values [9,15]. In dendrimers with carbazole dendrons (Ircarb)  $k_R = 5.6 \times 10^5 \text{ s}^{-1}$  is independent of generation, whereas the highly branched G1 dendrimer shows  $k_R = 3.7 \times 10^5 \text{ s}^{-1}$ . Lower values of  $k_R$  can be explained by a larger amount of ligand character in the predominantly metal-to-ligand charge transfer transition.

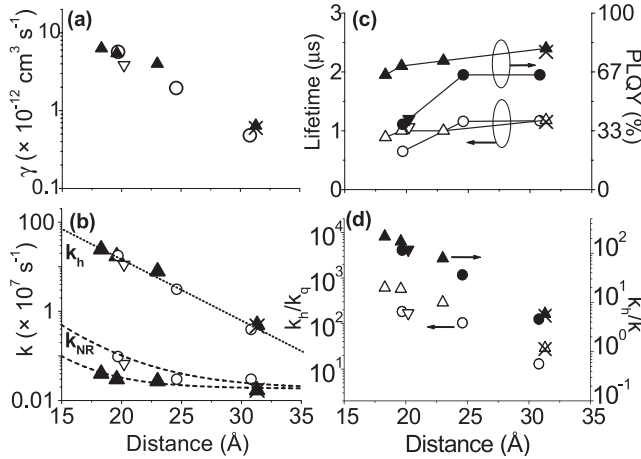


FIG. 2. Panel (a) shows the triplet-triplet annihilation rate as a function of the distance between Ir (ppy)<sub>3</sub> cores. Panel (b) shows the distance dependence of the hopping  $k_h$  and the nonradiative decay  $k_{NR}$  rates. The dotted line is the fit obtained with Eq. (2) and the dashed lines are fits by Eq. (3). Panel (c) displays PLQY and the PL lifetimes in the absence of annihilation with solid lines as guides for the eye. In panel (d) the ratios  $k_h/k_q$  (open symbols) and  $k_h/k$  (solid symbols) are plotted as a function of the distance between Ir (ppy)<sub>3</sub> cores. In these graphs, the upward pointing triangles are the data obtained from the neat film and the blends of Ir G1 in a CBP host, the crosses from the blend containing 20 wt% of Ir G1 in mCP, the circles from the neat films of the dendrimers Ircarb G1, G2, and G3, and the downward pointing triangles are from the highly branched G1 dendrimer.

The nonradiative decay rate  $k_{NR}$ , shown in Fig. 2(b), can be expressed as the sum of the nonradiative deactivation rate of isolated molecules,  $k_{NR-i}$ , and the quenching rate due to intermolecular interactions,  $k_q$ , so that  $k_{NR} = k_{NR-i} + k_q$ . Highly diluted dendrimers give  $k_{NR-i} = 1.8 \times 10^5 \text{ s}^{-1}$  for Ir G1 blends and Ircarb dendrimers, which indicates similar deactivation rates of isolated dendrimers. As shown in Fig. 2(b),  $k_{NR}$  can be described by:

$$k_{NR} = k_{NR-i} + \frac{1}{\tau} \left( \frac{R_0}{R} \right)^6, \quad (3)$$

where  $R_0$  is the Förster radius [16]. The best fit gives  $R_0 = 1.5 \text{ nm}$  for the Ir G1 blends and  $2 \text{ nm}$  for the neat films of Ircarb dendrimers, which is very similar to the Förster radius calculated from the spectral overlap of phosphorescence and absorption spectra of the Ir (ppy)<sub>3</sub> cores [9, 15]. The results show that  $k_q$  follows a dependence of  $R^{-6}$ . There is a recent report of this dependence in blends of Ir (ppy)<sub>3</sub> and it was ascribed to “dampening” of excitation energy by Förster type dipole-dipole interactions [9]. In the present work we show that the results can be explained by excitation transfer to a quencher.

Figure 2(d) shows that the triplet exciton hopping can be over 600 times faster than the phosphorescence quenching. We propose that transfer to the quencher is slow, limiting the quenching rate, and making the phosphorescence de-

cays insensitive to hopping rate. The decay would then be exponential with a rate of  $k_R + k_{NR-i} + k_q$ , where  $k_q$  is the transfer rate to the quencher [17]. Our results indicate that Dexter transfer to the quenchers is inefficient, which can be explained by a type II energy level offset between the emitter and quencher. The energy level offset would need to be sufficiently smaller than the exciton binding energy ( $\sim 1 \text{ eV}$ ) to prevent a quenching of the triplet excitons by charge transfer [18, 19] but large enough to make Dexter transfer to the quencher inefficient. Another possible explanation is that the highest occupied molecular orbital (HOMO) of the quencher is localized on the metal ion in contrast to the HOMO of the normal core, which is delocalized between the metal ion and ligands, so that the distance becomes too large for hole tunneling to the quencher. A possible quencher of this type is the *mer* isomer [20] which shows a higher HOMO energy with a more pronounced metal character than the *fac* isomer.

An average number of hops by an exciton during its lifetime is given by  $k_h/k$  where  $k = 1/\tau$  is the decay rate. The probability to visit the same site twice on a random walk in a 3D system is negligible. Therefore, the ratio  $k_h/k$  also represents the number of molecules sampled by triplet excitons. Figure 2(d) shows that this ratio varies from 220 in Ir G1 neat film to 5 in Ircarb-G3. Hence in all cases the migration of triplet excitons in Ir (ppy)<sub>3</sub>-cored dendrimers involves successive short range hops of the excitons between the cores until excitations decay radiatively or nonradiatively.

The results presented so far have all been for films with thicknesses in the range 170–200 nm. To gain a further insight into the phosphorescence quenching and exciton diffusion processes, we also studied the influence of the film thickness on the PL kinetics in Ir G1 and Ircarb-G1 neat films and in the blend containing 20 wt% of Ir G1 in CBP (Fig. 3). In both neat films, the PL decays were not significantly modified when the film thickness varied from 180 to 60 nm but a strong increase of the phosphorescence quenching when reducing the film thickness below 20 nm was observed. The dynamics of the exciton density in the case of quenching by an interface can be described by the diffusion equation:

$$\frac{\partial N(x, t)}{\partial t} = -\frac{N(x, t)}{\tau} + D \frac{\partial^2 N(x, t)}{\partial x^2}. \quad (4)$$

The boundary condition at the quenching interface is  $D \partial N(x, t) / \partial x = \nu N(x, t)$ , where  $\nu$  is the surface quenching velocity. The PL intensity is proportional to the exciton density integrated over the film thickness and, in the case of fast exciton diffusion ( $D \gg \nu d$  where  $d$  is the film thickness), is given by:

$$\int_0^d N(x, t) dx = N_0 d \exp \left[ -\left( \frac{1}{\tau} + \frac{\nu}{d} \right) t \right], \quad (5)$$

where  $N_0$  is the initial exciton density. As shown in Fig. 3(a) and 3(b), Eq. (5) describes our data well with

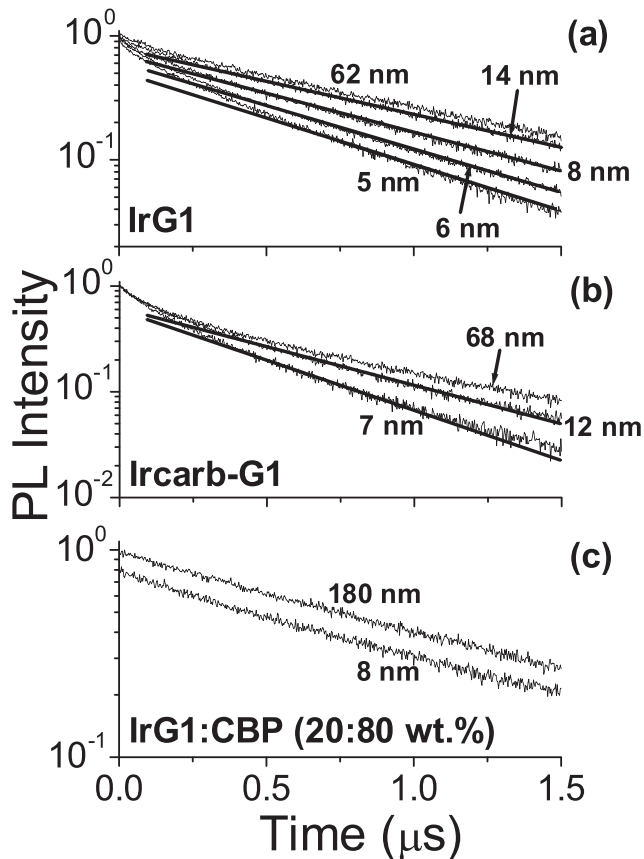


FIG. 3. PL kinetics of IrG1 neat film (a), Ircarb-G1 neat film (b), and the IrG1 : CBP (20:80 wt%) blend (c) for different film thicknesses at low excitation intensity. The decay curves in (c) are almost identical and have therefore been shifted vertically for clarity. Solid lines are the fits obtained using Eq. (5).

$v = 0.86 \text{ cm s}^{-1}$  for Ircarb-G1 and  $v = 0.35 \text{ cm s}^{-1}$  for IrG1, which shows that the phosphorescence quenching at the interface is more than twice as fast in Ircarb-G1. It is worth noting that this model does not fit the decay curves for films thicker than 20 nm which is to be expected as  $vd \sim D$ . These results suggest that there is quenching associated with one or both interfaces. The strength of the surface quenching was also found to be strongly dependent on the dielectric substrate used (data not shown) which suggests that the substrate-film interface is more likely to be responsible for this process. Additional experiments would be needed to clarify the mechanism of this surface quenching but we can already exclude the possibility that faster decays in thinner films could be due to an enhancement of dipole-dipole interactions because the overlap between absorption and emission spectra and hence Förster radius were independent of film thickness. Finally, we found that the PL decays in the IrG1 blend [Fig. 3(c)] with an average chromophore spacing of 3.1 nm (assuming a homogenous blend) are independent of the

film thickness. This result shows that the phosphorescence quenching at the surface can be totally suppressed by increasing the intermolecular distance between chromophores and thus reducing the exciton diffusion.

In summary, we have examined the PL properties of phosphorescent Ir(ppy)<sub>3</sub>-cored dendrimers with different molecular sizes in neat films and in blends. Triplet exciton diffusion rates obtained from triplet-triplet annihilation studies show exponential dependence on the spacing distance between phosphorescent cores in the range of 1.8 to 3.2 nm and an attenuation factor of  $0.33 \text{ \AA}^{-1}$ . This behavior confirms that triplet exciton diffusion is ruled by a Dexter mechanism. In contrast, the phosphorescence quenching rate in the volume of the films is governed by Förster type dipole-dipole interactions and is up to 615 times slower than the hopping rate. The direct comparison of these rates indicates that concentration quenching and triplet migration in Ir(ppy)<sub>3</sub>-cored dendrimers are different processes. The slower quenching than diffusion can be explained by a type II energy level offset between the emitters and quenchers. A different regime in which diffusion becomes important exists in very thin films ( $<20 \text{ nm}$ ) where additional quenching of triplet excitons is observed at the film surface and can be effectively overcome by increasing the intermolecular spacing between chromophores.

- [1] R. H. Friend *et al.*, *Nature (London)* **397**, 121 (1999).
- [2] R. J. Holmes *et al.*, *Org. Electron.* **7**, 163 (2006).
- [3] J. Kalinowski *et al.*, *Phys. Rev. B* **66**, 235321 (2002).
- [4] M. A. Baldo, C. Adachi, and S. R. Forrest, *Phys. Rev. B* **62**, 10967 (2000).
- [5] J. Kalinowski *et al.*, *J. Appl. Phys.* **98**, 063532 (2005).
- [6] M. A. Baldo, M. E. Thompson, and S. R. Forrest, *Nature (London)* **403**, 750 (2000).
- [7] C. Adachi, M. A. Baldo, and S. R. Forrest, *J. Appl. Phys.* **90**, 5048 (2001).
- [8] M. Ikai *et al.*, *Appl. Phys. Lett.* **79**, 156 (2001).
- [9] Y. Kawamura *et al.*, *Phys. Rev. Lett.* **96**, 017404 (2006).
- [10] D. L. Dexter, *J. Chem. Phys.* **21**, 836 (1953).
- [11] N. C. Greenham *et al.*, *Chem. Phys. Lett.* **241**, 89 (1995).
- [12] A. Suna, *Phys. Rev. B* **1**, 1716 (1970).
- [13] V. M. Agranovich and M. D. Galanin, *Electronic Excitation Energy Transfer in Condensed Matter* (Elsevier, New York, 1982), Vol. 3.
- [14] E. B. Namdas, A. Ruseckas, I. D. W. Samuel, S.-C. Lo, and P. L. Burn, *Appl. Phys. Lett.* **86**, 091104 (2005).
- [15] E. B. Namdas, A. Ruseckas, I. D. W. Samuel, S.-C. Lo, and P. L. Burn, *J. Phys. Chem. B* **108**, 1570 (2004).
- [16] T. Förster, *Discuss. Faraday Soc.* **27**, 7 (1959).
- [17] D. L. Huber, *Phys. Rev. B* **20**, 2307 (1979).
- [18] J. J. M. Halls *et al.*, *Phys. Rev. B* **60**, 5721 (1999).
- [19] A. C. Morteani *et al.*, *Phys. Rev. Lett.* **92**, 247402 (2004).
- [20] A. B. Tamayo *et al.*, *J. Am. Chem. Soc.* **125**, 7377 (2003).